

Water Resources Research

RESEARCH ARTICLE

10.1029/2019WR025658

Key Points:

- Baseflow-specific discharge increased more than threefold as catchment area increased from 0.05 to 93.58 km² in a steep headwater
- A large amount of water infiltrated into bedrock in hillslopes in the headwater area and was only added to the river further downstream
- Storage and discharge in mesoscale catchments can be assessed based on simple area baseflow-specific discharge relationships

Supporting Information:

- Supporting Information S1

Correspondence to:

Y. Asano,
yasano@uf.a.u-tokyo.ac.jp

Citation:

Asano, Y., Kawasaki, M., Saito, T., Haraguchi, R., Takatoku, K., Saiki, M., & Kimura, K. (2020). An increase in specific discharge with catchment area implies that bedrock infiltration feeds large rather than small mountain headwater streams. *Water Resources Research*, 56, e2019WR025658. <https://doi.org/10.1029/2019WR025658>

Received 11 JUN 2019

Accepted 21 JUL 2020

Accepted article online 23 JUL 2020

An Increase in Specific Discharge With Catchment Area Implies That Bedrock Infiltration Feeds Large Rather Than Small Mountain Headwater Streams

Yuko Asano¹ , Masatoshi Kawasaki², Toshihiro Saito¹, Ryusei Haraguchi¹, Kae Takatoku¹, Michio Saiki¹, and Kota Kimura³

¹The University of Tokyo Chichibu Forest, Graduate School of Agricultural and Life Sciences, The University of Tokyo, Saitama, Japan, ²Institute for Water Science, Suntory Global Innovation Center Limited, Kyoto, Japan, ³The University of Tokyo Hokkaido Forest, Graduate School of Agricultural and Life Sciences, The University of Tokyo, Hokkaido, Japan

Abstract Mountains are a source of water for downstream areas; thus, it is important to understand the storage and discharge characteristics of steep mountain catchments. Nested catchment studies have indicated that the relation between catchment area and specific discharge during baseflow can represent mesoscale storage and discharge characteristics, but this is poorly understood. We found that baseflow-specific discharge increased with catchment size in the headwater of the Arakawa River and identified the processes responsible for this spatial pattern. Synoptic discharge measurements obtained in catchment areas of 0.05 to 93.58 km² showed that specific discharge increased more than threefold with increasing drainage area. Analyses of the spatial variation in precipitation, hydrographs from three continuous gauging stations, and isotopic tracers implied that in this catchment, considerable amounts of water infiltrated in bedrock on hillslopes and did not discharge into small streams, but instead fed surface flow into a larger downstream catchment. A review of previous nested studies demonstrated three spatial patterns for specific discharge: Specific discharge may increase or decrease with catchment area, or it may be independent of area. An increase in specific discharge with area was observed only in catchments with permeable bedrock, which implies that such an increase is a useful indicator of the importance of the bedrock flow path to mountain watershed storage. The pattern of relationships between catchment area and specific discharge can be used to assess the storage and discharge properties of mesoscale catchments when the processes driving each pattern have been clarified.

1. Introduction

In many regions, mountains are a source of water for downstream ecosystems and society. Therefore, characterizing the storage and discharge of mesoscale mountain catchments (10⁰–10³ km²) is important. It is often more difficult to understand processes in mesoscale catchments than in smaller catchments, because it is difficult to conduct sufficiently detailed measurements to characterize the internal flow system of a catchment, except at a few intensively studied sites (e.g., Didszun & Uhlenbrook, 2008; Sayama et al., 2011). The relationship between catchment area and the pattern in the runoff response to rainfall can elucidate catchment processes (e.g., Asano et al., 2018; Blöschl & Sivapalan, 1997; Egusa et al., 2019; Soulsby et al., 2009; Temnerud et al., 2007). The main landscape units that contribute to baseflow may shift from hillslope soil to bedrock, riparian areas, or other features as the catchment area increases (e.g., Gomi et al., 2002). The dominant mechanism of runoff storage and generation differs among landscape units, favoring lateral subsurface flow in hillslope soil (Tromp-van Meerveld & McDonnell, 2006; Tsuboyama et al., 1994), flow through weathered or fractured bedrock or unconsolidated deposits (e.g., Anderson et al., 1997; Katsuyama et al., 2010; Kosugi et al., 2008; Roy & Hayashi, 2009; Uchida et al., 2008), or exchange with the riparian zone (e.g., Laudon & Sponseller, 2018), and therefore the runoff response may change with catchment size. Integrating information about the relationship between the spatial pattern of the hydrologic response and internal processes is useful, but such studies remain limited. In addition, spatial heterogeneity in yield can exist even among catchments of the same size consisting of the same landscape units, for example, due to a spatially heterogeneous distribution of vegetation, soil type, or depth (e.g., Lyon et al., 2012). Variability among similar-sized catchments often decreases with an increase in catchment area of about

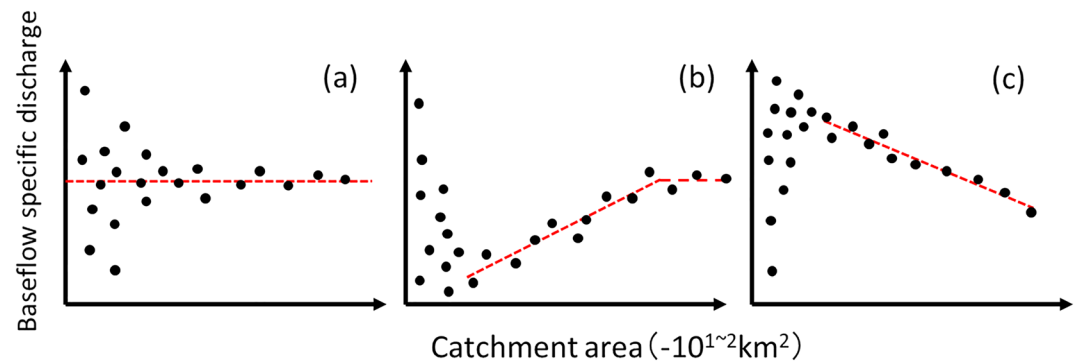


Figure 1. Schematic diagram of spatial patterns in baseflow-specific discharge as a function of catchment area: (a) constant independent of catchment area, (b) increasing with greater catchment area, and (c) decreasing with greater catchment area.

1 km², mostly through the mixing that occurs in stream networks when tributaries merge with one another and with the main stream (e.g., Asano & Uchida, 2010; Wood et al., 1988, 1995).

In this study, we focused on baseflow changes with catchment scale to better understand the storage and discharge properties of a mountain catchment. Three general spatial patterns in yield have been reported in previous studies of nested catchments involving extensive baseflow measurements across mesoscale catchments in relatively steep terrain. The nested design allows the measurement of multiple longitudinal upstream-to-downstream profiles within a stream network. The first pattern observed in such studies is that specific discharge is almost constant and independent of catchment area for areas up to about 100 km² (Figure 1a; see also Asano et al., 2009; Lyon et al., 2012; Wood, 1995). The second pattern is that specific discharge increases with catchment area (Figure 1b; e.g., Fujimoto et al., 2016; Shaman et al., 2004), presumably because of the contribution of groundwater flow paths, as demonstrated theoretically by Tóth (1963). The third pattern is a decrease in specific discharge with catchment area during low-flow conditions (Figure 1c; Floriani et al., 2019; Tetzlaff & Soulsby, 2008). Many of the studies that have demonstrated independent, increasing, or decreasing trends in specific discharge with increased catchment size have also found highly variable specific discharge in smaller catchments (0.1–1 km²) that show no coherent pattern with catchment area, whereas larger catchments tend to show less variation (e.g., Tetzlaff & Soulsby, 2008; Woods et al., 1995).

In this study, we focused on the pattern of increasing specific discharge with catchment area (Figure 1b). Previous studies using geochemical tracers have shown that an increase in specific discharge is associated with increased deep groundwater/bedrock groundwater exfiltration (Egusa et al., 2016; Fujimoto et al., 2016; Shaman et al., 2004), which is less significant or absent in smaller catchments. Groundwater in weathered or fractured bedrock can contribute substantially to the response of runoff to rainfall in small catchments in steep headwaters (e.g., Anderson et al., 1997; Komatsu & Onda, 1996; Onda et al., 2001, 2006; Uchida et al., 2003). Bedrock permeability is the key parameter controlling the storage and discharge properties of mesoscale catchments (e.g., Hale & McDonnell, 2016; Peralta-Tapia et al., 2015; Pfister et al., 2017; Sayama et al., 2011; Tetzlaff & Soulsby, 2008). Specifically, low flow-specific discharge increases with catchment area between 1 and 10 km² (Egusa et al., 2016) and between 0.3 and 3 km² (Fujimoto et al., 2016) and is similar among catchments with areas larger than 4 km² (Fujimoto et al., 2016) and above a critical basin size of 8 to 21 km² (Shaman et al., 2004). These findings imply that specific discharge increases up to a critical catchment size, but after a stream has passed through the majority of the deeper flow paths recharged by higher elevation subcatchments, specific discharge cannot increase further unless groundwater is transferred across the catchment boundary. Beyond this critical catchment size, the relation between specific discharge and catchment area should become almost constant if precipitation and evapotranspiration are constant (Figure 1b). Identifying this critical size for catchments that exhibit increasing specific discharge with area is important.

The relationship between specific discharge and catchment area can provide insights into storage and discharge characteristics in steep mesoscale catchments, in particular the contribution of deep groundwater; however, limited information is available on the catchment conditions that generate an increase in

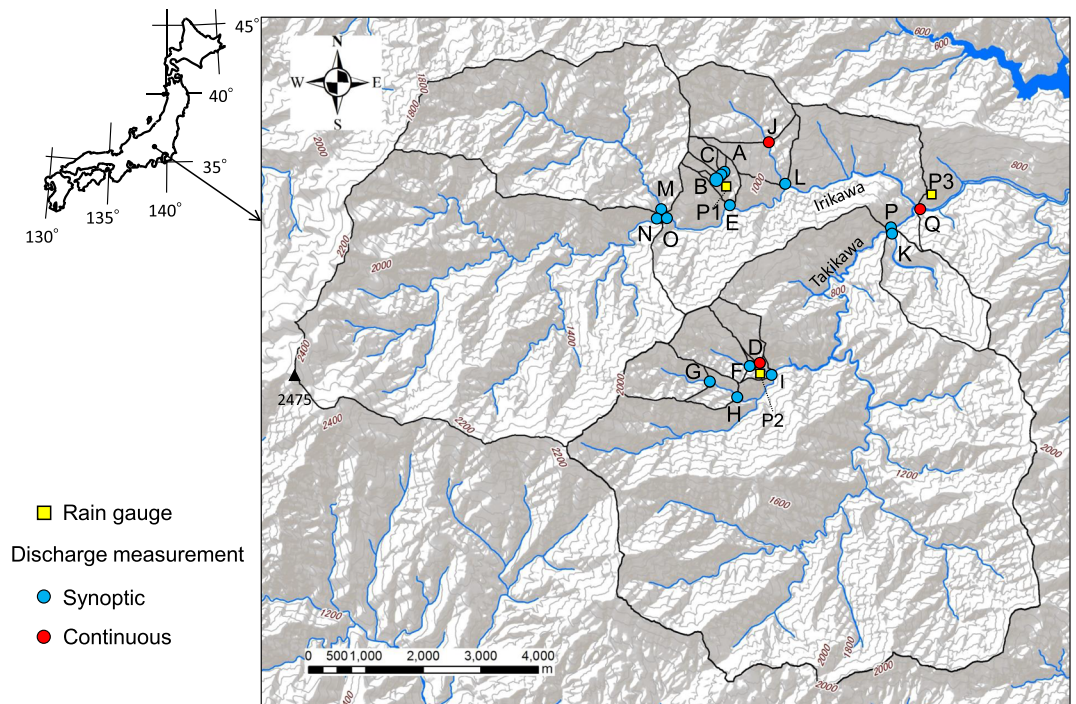


Figure 2. Location and topography of the studied watershed in the headwater of the Arakawa River in the Okuchichibu Mountains. Locations of rain gauges and discharge measurements are shown.

specific discharge with area. Furthermore, the increase in specific discharge with increasing catchment size in a steep catchment is likely caused by a commensurate increase in the contribution of deep groundwater (e.g., Egusa et al., 2016; Shaman et al., 2004), but other causes are possible. Spatial variation in precipitation affects stream flow (e.g., Singh, 1997), although these effects have not been tested for the relationship between area and specific discharge in mesoscale catchments. Decreases in peak event flow-specific discharge with catchment area have also been demonstrated (e.g., Furey & Gupta, 2005; Ogden & Dawdy, 2003). Peak flow can be partitioned into quick flow and baseflow component, if this above reduction in peak flow with area were to coincide with a reduction in the quick flow component of the storm response, which would indicate that more water is being partitioned into baseflow. Storm flow can be partitioned into quick flow and baseflow component. If this is the case, an increase in baseflow with area might be observed, although the total annual flow level would remain similar. The possible effects of systematic changes in the partitioning of precipitation into flood quick flow and baseflow with catchment area have not been evaluated in terms of the relationship between area and specific discharge.

In this study, we characterized the increase in specific discharge with catchment area during baseflow conditions and infer the mechanisms likely underlying this relationship in our study catchment. We conducted synoptic discharge measurements at the outlets of catchments ranging from 0.05 to 93.58 km² in size in the headwaters of the Arakawa River in Japan, where specific discharge increases with catchment area. To clarify the mechanisms underlying the observed scale-dependent pattern, we tested three hypotheses using different scenarios with respect to the cause of increasing specific discharge, using both hydrometric and stable isotope measurements:

- a. A considerable amount of precipitation that infiltrates into bedrock in hillslopes does not return to surface flow within the topographic area of a small catchment but instead is discharged downstream into the streams of larger catchments.
- b. Spatial patterns in precipitation are responsible for the observed increase in specific discharge with area.
- c. In a small catchment, discharge disproportionately occurs via event flow relative to a larger catchment; thus, during baseflow, the measured discharge in a smaller catchment is less than that in a larger catchment, whereas the total annual flow remains similar.



Figure 3. Photos of streams measured with gauging instruments at (a) Location D, (b) Location J, (c) Location Q, and (d) the discharge measurement at Location N.

We also reviewed previous studies that demonstrated area-specific discharge relationship and identified the catchment size and properties that required for the characteristic spatial pattern to appear.

2. Study Site

The study catchments were Irikawa and Takikawa, which are located in the University of Tokyo Chichibu Forest in Saitama Prefecture, Japan (Figure 2). The area is located in the headwater of the Arakawa River in the Okuchichibu Mountains. The Arakawa River runs through Tokyo to Tokyo Bay. As a result of erosion and the formation of a V-shaped valley by the Arakawa River, slopes in the area are very steep, in particular in the lower portions along the valleys. The mean slope of the entire catchment is 67%; therefore, the small tributaries that run into the main valleys flow down like a cascade (Figure 3). The channels are classified morphologically as cascades, step-pools, or plane beds according to Montgomery and Buffington (1997), and all have small flood plains and riparian areas (Figure 3). The stream channels in the study area range from first to sixth order stream according to Strahler (1952). Bedrock exposure along channels can be observed, in particular in the lower portions of tributaries where they enter the main valleys and in the main channels. Channel beds are composed of large rocks, loose boulders, and gravel. Thus, some hyporheic underflow should exist in the study area. The elevation of the catchment ranges from 628 to 2,475 m above sea level. There are no glaciers within the catchments.

The bedrock in the study area consists mainly of Cretaceous Shimanto accretionary complex and Jurassic Chichibu accretionary complex (Figure S1; Hara et al., 2010). The peaks in the catchment (Kobushigatake) consist of granodiorite. Some faults have been reported in this area, including the Hakutai Danso fault (Chichibu Geologic Research Group, 1966), and fractures are observed at outcrops. Soil depth can be less than 1 m on the steep slopes, but gentle ridges are covered with 2 to 3.2 m of the Kanto loam formation, which is mostly weathered tephra deposited between 8×10^4 and 1.5×10^4 years ago (Chichibu Geologic Research Group, 1966). The soil is mostly Cambisols (brown forest soil).

The mean annual precipitation between 2002 and 2016 was 1,494 mm, and the mean annual temperature was 11.1°C at Location P3 (Figure 2; Meteorology Division, Fundamental Data Development Committee, University of Tokyo Forests, 2018). Precipitation occurs throughout the year in the area, mostly during the two rainy seasons from June to July and September to October. Precipitation in winter is limited (Figure 4a). In 2013 and 2014, for example, 73% of annual rainfall occurred in the 5 months between June and October. The maximum instantaneous snow depth varies annually from 0.2 to 0.3 m, and snow generally melts within 1 to 2 weeks of falling in most areas of the catchment.

The catchment covers from montane to subalpine vegetation zones. The whole area is covered by plantations and secondary and natural primary forests with closed canopies. Planted species include *Chamaecyparis obtusa*, *Larix kaemferi*, and *Cryptomeria japonica*. The secondary and natural primary forests mainly consist of deciduous hardwoods such as *Fagus crenata*, *Fagus japonica*, *Fraxinus platypoda*, and *Pterocarya rhoifolia* as well as conifers such as *Tsuga sieboldii*, *Abies firma*, *Chamaecyparis obtusa*, *Tsuga diversiflora*, and *Abies veitchii*.

Evapotranspiration from forest areas in central Japan has been estimated to be around 600–900 mm/year (Kondo et al., 1992; Sawano et al., 2015), and evapotranspiration from the upstream portion of the Arakawa catchment (Yorii, area of 927 km² including city and residential areas, but mostly forest) has been measured at 500 mm based on annual water budget (Saitama Prefecture, 1987). These estimates imply that one third to half of annual precipitation returns to the atmosphere rather than ultimately discharging into the stream in this catchment.

In central Japan, published estimates of the isotopic lapse rate, which is the depression of isotopic δ values per unit increase in elevation based on precipitation observations, show an arithmetic mean of -2.086‰ km^{-1} (Yamanaka et al., 2016). Multiple regression analyses that consider latitude and longitude in addition to elevation have shown an isotopic lapse rate of -1.724‰ km^{-1} (Yamanaka et al., 2015). The sites of those studies in central Japan were located within about 150 km of our study site, and their elevations ranged from 0 to 3,750 m, with elevation ranges in individual studies of 500 to 3,690 m.

3. Methods

3.1. Measurement of Synoptic Baseflow Discharge

Measurement locations were selected based on accessibility and previous monitoring. On 27–28 October 2011, preliminary discharge measurements were conducted at 22 sites in smaller streams and larger streams that could be waded. The size of the topographic catchment areas draining toward the measurement locations ranged from 10^{-4} to 10^1 km². We found that in catchments smaller than 10^{-1} km², specific discharge varied by almost three orders of magnitude (0.1–97 mm/day), and specific discharge clearly increased with catchment size (from 0.12 to 3.5 mm/day) when the catchment area exceeded about 0.05 km² (Asano et al., 2013). To focus on the size-dependent increase, we selected 13 locations with areas larger than 0.05 km² according to their accessibility at the time of sampling. We conducted synoptic surveys on 31 May and 22 August in 2013, and data from three synoptic surveys, including the preliminary measurements in October 2011, were used for analyses (Table 1). The catchment areas of the selected sites ranged from 0.05 to 93.58 km², with elevations ranging from 628 to 1,285 m asl (above sea level; Table 1). Synoptic discharge measurements were collected under relatively stable flow conditions during a period with no precipitation (Figure 4a). We were able to take measurements at 11 to 13 locations during each campaign. Hourly discharge at gauging station Q varied by 5% to 8% during each of the three synoptic measurement campaigns. Hourly discharge at gauging station D varied by 22% and 48% during two synoptic measurement campaigns conducted in 2013.

Discharge was measured with a plastic bag, stopwatch, and weight scale at locations where flow was less than about 1 L/s. At higher discharge rates or in larger channels, we measured discharge using the velocity-area gauging method (Figure 3d). We determined the cross-sectional area by measuring water depths at intervals of 0.05 to 0.5 m over the entire stream width, depending on width and bed morphology, and measured flow velocity at each location at 60% of the total water depth from the surface. Based on repeated measurements at location L, the error was assumed to be less than 10%. For locations with a weir and fixed monitoring station, hourly discharge measured at 12:00 was multiplied by 24 and presented as

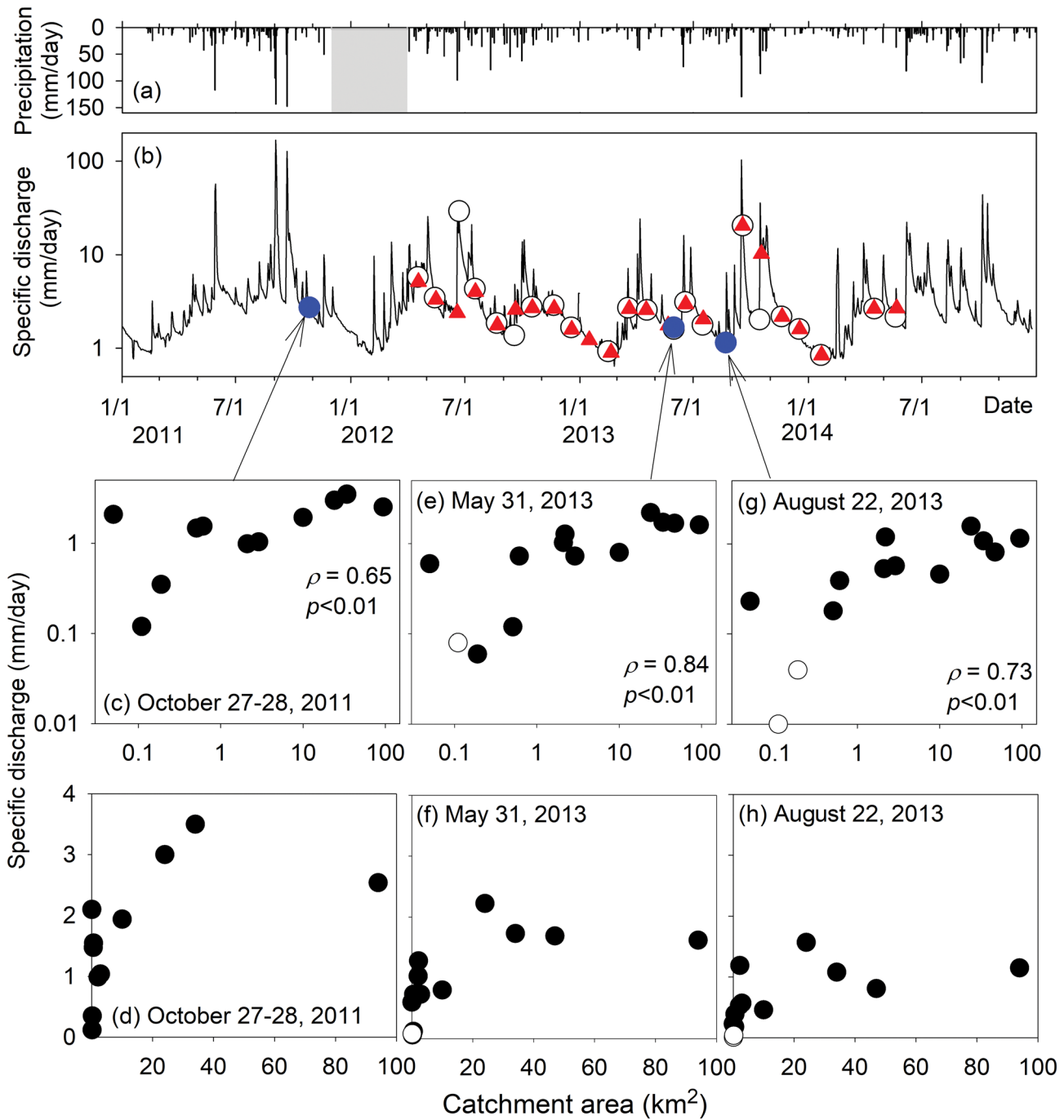


Figure 4. (a) Daily precipitation measured at P3 (missing data from 1 December 2011 to 31 March 2012). (b) Daily discharge measured at Location Q for 2011 to 2014. Blue circles indicate synoptic discharge measurements; open circles show isotope sampling times at Locations A, B, C, E, J, L, M, N, and O; and red triangles show isotope sampling times for Locations D, F, G, H, I, K, and P. (c–h) Relationships between catchment area and measured specific discharge during baseflow on (c, d) 27–28 October 2011, (e, f) 31 May 2013, and (g, h) 22 August 2013, respectively. Panels (c), (e), and (g) have log scales for both axes, with ρ indicating a significant Spearman rank correlation ($p < 0.05$), whereas (d), (f), and (h) show the same data at linear scale. Plots with open circles show discharge that was evaluated visually and was not used for statistical analyses.

daily specific discharge (mm/day) for comparison (Figures 3a–3c). In addition, when the water flow was so low that we could not use the plastic bag method described above, we visually estimated the discharge. These data are noted in figures and were not used for statistical analyses.

Table 1
The Areas, Slopes, and Elevations of the Studied Catchments and Measurements Conducted at Each Location

| Location ID | Catchment area (km ²) | Mean slope (%) | Elevation of catchment (m) | | | Synoptic discharge measurement | Continuous discharge measurement | Isotope measurement |
|-------------|-----------------------------------|----------------|----------------------------|---------|-------|--------------------------------|----------------------------------|---------------------|
| | | | Lowest | Highest | Mean | | | |
| A | 0.05 | 50 | 1,133 | 1,352 | 1,254 | ○ | - | ○ |
| B | 0.11 | 49 | 1,129 | 1,491 | 1,349 | ○ | - | ○ |
| C | 0.19 | 49 | 1,126 | 1,549 | 1,377 | ○ | - | ○ |
| D | 0.51 | 56 | 1,038 | 1,646 | 1,388 | ○ | ○ | ○ |
| E | 0.61 | 55 | 811 | 1,549 | 1,241 | ○ | - | ○ |
| F | 1.02 | 66 | 1,079 | 1,781 | 1,442 | - | - | ○ |
| G | 1.10 | 69 | 1,285 | 2,010 | 1,713 | - | - | ○ |
| H | 1.45 | 71 | 1,155 | 2,023 | 1,631 | - | - | ○ |
| I | 1.66 | 63 | 929 | 1,790 | 1,404 | - | - | ○ |
| J | 2.09 | 66 | 941 | 1,791 | 1,347 | ○ | ○ | ○ |
| K | 2.20 | 70 | 657 | 1,761 | 1,216 | ○ | - | ○ |
| L | 2.93 | 61 | 739 | 1,791 | 1,270 | ○ | - | ○ |
| M | 10.48 | 65 | 917 | 1,991 | 1,457 | ○ | - | ○ |
| N | 24.01 | 65 | 914 | 2,475 | 1,707 | ○ | - | ○ |
| O | 34.49 | 65 | 914 | 2,475 | 1,631 | ○ | - | ○ |
| P | 47.36 | 70 | 653 | 2,287 | 1,467 | ○ | - | ○ |
| Q | 93.58 | 67 | 628 | 2,475 | 1,479 | ○ | ○ | - |

Specific discharge (mm/day) was calculated based on the measured discharge and the catchment area obtained from topographical analyses shown in section 3.3. We calculated Spearman rank order correlations between the catchment area and specific discharge.

The mean elevations of the catchments draining to the measurement locations was small (1,216–1,707 m) relative to the large elevation range in the catchment (628–2,475 m; Table 1, Figure S2). Smaller catchments tended to have lower mean elevations than the larger catchment, but the regression analysis between catchment area and mean elevation of the measurement location gave small coefficient of determination ($r^2 = 0.27$, $p < 0.1$).

3.2. Measurement of Continuous Discharge

Discharge was measured continuously at three locations, D, J, and Q (Figures 2 and 3), with a rectangular weir at Location D (Bakemonosawa; Kimura et al., 2015; Figure 3a) and an erosion control dam at Location J (Yatakezawa; Asano et al., 2017; Figure 3b). Those structures were built on the bedrock. At Location Q, discharge was measured hourly by the Ministry of Land, Infrastructure, Transport and Tourism of Japan (Kawamata, location ID 303041283320010; Ministry of Land Infrastructure, and Transport and Tourism of Japan, Water Information System, n.d.; Figure 3c). There is a water intake about 200 m upstream of Location Q for a run-of-the-river hydroelectric power plant. Thus, we summed the monitored discharge data at Location Q and the water intake data monitored by the Tokyo Electric Generation Company, Inc. (Tokyo, Japan), to determine the original discharge at Location Q. Because of sediment movement and filling of pools, discharge measurements were frequently interrupted, in particular at Location J. For hydrograph comparison, we used data acquired in 2014, for which we had more data than other years.

3.3. Measurement of Precipitation

To understand the spatial variation in precipitation, we measured precipitation outside of the freezing period using a tipping-bucket rain gauge (0.5 mm per tip) located in open areas at Locations P1 (1,210 m asl), P2 (1,080 m asl), and P3 (740 m asl; Figure 2). We compared precipitation levels measured over a total of 8 months (April–November) in 2012 to 2014. To understand the differences in wetness conditions among measurement campaigns, we calculated the 10-day antecedent rainfall prior (API_{10}) using precipitation measured at P2 (Kohler & Linsley, 1951).

Our rain gauge locations covered a limited range of elevations within the catchment (Figure S2), although precipitation increases almost linearly with elevation in the mountains (e.g., Yamada et al., 1995). To compensate for this limitation in our measurements, we used a 1-km² mesh of 30-year (1981–2010) normal

Table 2
Observed Specific Discharge From the Three Surveys and Calculated Areal Mean Normal Annual Precipitation at Each Location

| Location ID | Specific discharge (mm/day) | | | | Catchment mean normal annual precipitation (mm) |
|-------------|-----------------------------|-------------|----------------|---------|---|
| | 27–28 October 2011 | 31 May 2013 | 22 August 2013 | Average | |
| A | 2.1 | 0.60 | 0.23 | 0.96 | 1,565 |
| B | 0.12 | 0.08 | 0.01 | 0.07 | 1,565 |
| C | 0.35 | 0.06 | 0.04 | 0.15 | 1,565 |
| D | 1.5 | 0.12 | 0.18 | 0.59 | 1,585 |
| E | 1.5 | 0.73 | 0.39 | 0.89 | 1,573 |
| F | - | - | - | - | 1,586 |
| G | - | - | - | - | 1,588 |
| H | - | - | - | - | 1,589 |
| I | - | - | - | - | 1,586 |
| J | 0.99 | 1.03 | 0.53 | 0.85 | 1,525 |
| K | - | 1.28 | 1.19 | 1.23 | 1,603 |
| L | 1.0 | 0.73 | 0.57 | 0.78 | 1,532 |
| M | 1.9 | 0.80 | 0.46 | 1.07 | 1,535 |
| N | 3.0 | 2.22 | 1.57 | 2.27 | 1,574 |
| O | 3.5 | 1.73 | 1.08 | 2.09 | 1,561 |
| P | - | 1.69 | 0.81 | 1.25 | 1,616 |
| Q | 2.7 | 1.62 | 1.15 | 1.83 | 1,589 |

Note. Unit discharges in italics were visually estimated values. Columns with “-” show no measurement conducted. Catchment mean normal annual precipitation was calculated based on 30-year normal annual precipitation.

annual precipitation data (we call as “normal annual precipitation” thereafter) provided by the Japan Meteorological Agency (1981–2010). These data were estimated based on multiple regression analyses of mean precipitation at the monitoring locations and topographic factors such as elevation and slope using data from about 1,256 meteorological stations and Automated Meteorological Data Acquisition System stations observed between 1981 and 2010. Using these data, we calculated the areal mean normal annual precipitation for the area upstream of each measurement location. Spearman’s rank correlations were calculated between the catchment mean normal annual precipitation value for each measurement location and the specific discharge measured during each synoptic survey to test the effects of variability in precipitation on the spatial pattern of specific discharge.

3.4. Topographical Analyses

A 10-m digital elevation model (DEM) was used to calculate the mean elevation, area, and slope of each catchment draining to the discharge measurement locations. The DEM was provided by ESRI Japan Corp. (Tokyo, Japan). The analyses were performed with ArcGIS 10.6 with the Spatial Analyst extension. First we created the watershed boundary for each location using the hydrology toolset with a basic D8 flow direction algorithm. Then we calculated the slope at each location using the slope toolset. After creating the watershed boundary, we calculated catchment areas using the Calculate Geometry tool. Mean elevation and mean slope were calculated with the Zonal Statistics tool.

3.5. Measurement of Stable Isotope Tracers in Water

3.5.1. Water Sampling and Isotope Measurements

We used stable isotopes of water ($\delta^2\text{H}$ and $\delta^{18}\text{O}$) to determine the recharge elevation of water for the streams. Grab samples of stream water were collected monthly from April 2012 to March 2014 at all locations except Location Q in Figure 1 (Table 2). Water sampling was conducted primarily during low-flow conditions, when baseflow was presumed to be dominant, but a few high-flow samples were included (Figure 4a).

Rainfall collectors were installed to collect rainwater at Location P2 (Figure 2). They consisted of bottles fitted to funnels with a diameter of 24 cm between April and October or May and November and 38.5 cm at other times. Rainfall samples were collected monthly.

All rainfall and stream water samples were analyzed for their isotopic composition at the Laboratory of Isotope Geochemistry at the University of Arizona (Tucson, AZ, USA). For $\delta^2\text{H}$ analyses, samples were reduced with Cr metal at 750°C and analyzed with an H-Device attached to a mass spectrometer (MAT Delta-S; Finnigan, Hemel Hempstead, UK). For $\delta^{18}\text{O}$ analyses, samples were equilibrated with CO_2 gas at approximately 15°C in an automated equilibration device coupled to the same mass spectrometer. The results were calibrated according to the composition of the V-SMOW and SLAP isotopic reference materials. The analytical precision of the $\delta^2\text{H}$ and $\delta^{18}\text{O}$ measurements was $\pm 0.9\text{‰}$ and $\pm 0.08\text{‰}$, respectively.

3.5.2. Evaluation of the Effects of Evaporative Fractionation

The effects of evaporative fractionation on stream samples were assessed through comparison with the local meteoric water line on a dual isotope plot of precipitation and stream isotopic composition (e.g., Craig, 1961).

We calculated the local meteoric water line (LMWL) through regression of the dual isotope plot and comparison with the Global Meteoric Water Line (GMWL) with a slope of 8 (Dansgaard, 1964), expressed as

$$\delta^2\text{H} = 8 \times \delta^{18}\text{O} + d. \quad (1)$$

Table 3
Total Precipitation (mm) Measured Between April and November at P1, P2, and P3 and Annual Precipitation Measured at P3

| Rain gauge ID | Elevation (m) | Year | | |
|--|---------------|-------|-------|-------|
| | | 2012 | 2013 | 2014 |
| <i>Precipitation measured between April and November</i> | | | | |
| P1 | 1,210 | 1,303 | 1,182 | 1,272 |
| P2 | 1,080 | 1,480 | 1,247 | 1,332 |
| P3 | 740 | 1,335 | 1,132 | 1,210 |
| <i>Annual precipitation</i> | | | | |
| P3 | 740 | - | 1,281 | 1,440 |

Note. “-” indicates no data.

If stream water aligned with this LMWL, we assumed that the effects of isotopic fractionation through evaporation were minimal. We constructed separate LMWLs for the wet (June–October) and dry (all other months) seasons to assess the effects of evaporative fractionation over 1-month collection periods during both seasons.

3.5.3. Using the Isotopic Lapse Rate to Determine Recharge Elevation

In mountain regions in central Japan, long-term (a year to several years) mean stable isotope ratios in precipitation are strongly affected by elevation (e.g., Waseda & Nakai, 1983; Yamanaka et al., 2015), similar to other mountain regions worldwide (e.g., Clark & Fritz, 1997; Liebminger et al., 2006). The effects of elevation on precipitation and isotopic lapse rates calculated from long-term mean values can be considered nearly constant within a given mountain

region (e.g., $<10^2$ km²; Yamanaka et al., 2015, 2016). Temporal variation in the isotopic composition of precipitation is large, but variation in the isotopic composition of stream water is generally small, reflecting mixing and dispersion during subsurface flow processes (e.g., Waseda & Nakai, 1983; Yamanaka et al., 2016). To determine the recharge elevation of each stream, we compared the mean elevation of each catchment with the mean $\delta^{18}\text{O}$ of stream water (based on monthly sampling; e.g., Clark & Fritz, 1997; Peters et al., 2018). If all residuals of precipitation minus evapotranspiration in the catchment contributed equally to streamflow, the stream isotopic composition should have reflected the known elevation effect.

4. Results

4.1. Relationships Between Catchment Area and Specific Discharge During Baseflow

We observed a statistically significant (at a threshold of $p < 0.05$) monotonic increase in specific discharge with respect to catchment area for data obtained during all three measurement campaigns, although the data showed notable scatter (Figures 4c–4h). For example, the mean specific discharge of catchments with areas greater than 10 km² was more than three times that of catchments with areas smaller than 1 km² in all three campaigns. Plots on an arithmetic scale showed that the increase in specific discharge was unclear for catchment areas greater than 20–30 km² (Figures 4d, 4f, and 4h), although only three to four measurement locations were sampled and the data were scattered. Meanwhile, specific discharge for the smallest location, A (0.05 km²), was high for its catchment area and deviated from the general trend, in particular for the October 2011 and May 2013 sampling points. In addition, specific discharge was almost twice as great at Location K (2.2 km²) than at Location L (2.9 km²), although their catchment areas were similar (Table 2).

Discharge was largest in October 2011 and smallest in August 2013, reflecting the wetness conditions of the individual measurement campaigns (Figures 4a and 4b). The API₁₀ values were 6.9, 4.2, and 3.2 mm for October 2011, May 2013, and August 2013, respectively. Although the wetness conditions of the catchment changed, the general trend of increasing specific discharge with area was consistent.

4.2. Spatial Distribution of Precipitation

Eight-month total precipitation was largest at P2 (1,080 m asl) and smallest at P3 (740 m asl) in all 3 years (Table 3). The differences in total 8-month precipitation at the three rain gauges were 115–145 mm, which were 11% to 13% of the mean 8-month precipitation. Monthly precipitation showed similar seasonal trends at all three locations (Figure S3). The mesh of 30-year normal annual precipitation ranged from 1,489 to 1,656 mm within the study area, and the calculated catchment mean normal annual precipitation ranged from 1,525 mm (Location K) to 1,616 mm (Location P; Table 2). The differences in normal annual precipitation among mesh grids and among catchments were small, with maximums of 10% and 6%, respectively. Furthermore, no statistically significant ($p < 0.1$) relationships between catchment mean normal annual precipitation and the specific discharge of catchments were found for any of the measurement campaigns (Figure S4).

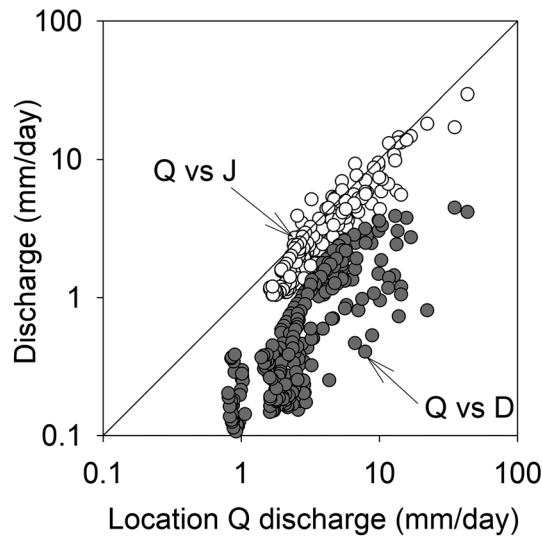


Figure 5. Comparison of discharge measurements in 2014 at Location Q (93.58 km²) on the x axis and at Locations J (2.09 km²) and D (0.51 km²) on the y axis.

$p < 0.01$) overlapped, and both were characterized by slopes 98 and 86% of the slope 8 of GMWL, although their data showed some scatter (Figure 6). This result showed that effects of evaporative fractionation over the 1-month collection period were small. The slope of 6.9 for the dry period was 12% smaller than that for the wet period, which showed that precipitation samples during the dry period were more affected by evaporative fractionation than that during the wet period. The stream water samples fell within a narrow range and were mostly within the 95% confidence intervals of the regression lines during both the wet and dry periods (Figures 6a and 6b).

There was marked temporal variation in the $\delta^{18}\text{O}$ and $\delta^2\text{H}$ ratios of precipitation (Table 4, Figure S6). Streams under baseflow conditions showed very small temporal variation (Table 4, Figure S6). The $\delta^{18}\text{O}$ in precipitation ranged from -6.1‰ to -17.0‰ , whereas that in streams ranged from -10.0‰ to -11.8‰ . The standard deviation of $\delta^{18}\text{O}$ in precipitation was 2.6‰ , whereas the corresponding value in stream water was almost one order of magnitude smaller, with a range from 0.10‰ to 0.32‰ (Table 4). The standard deviations of $\delta^{18}\text{O}$ in streams were close to the analytical precision of measurement ($\pm 0.08\text{‰}$).

4.5. Isotope Ratios Along an Elevation Gradient

Mean $\delta^{18}\text{O}$ decreased with the mean elevation of the catchment, although there was significant scatter in the relationship (Figure 7). The slope of the linear regression showed an isotopic lapse rate of -1.8‰ km^{-1} ($r^2 = 0.60$, $p < 0.01$), which was similar to the reported average isotopic lapse rate in central Japan (Yamanaka et al., 2015, 2016). Mean $\delta^{18}\text{O}$ values fell within a narrow range from -11.36 to -10.49 . Consequently, the ranges of temporal isotopic fluctuation overlapped, although temporal fluctuations were small for each location (Table 4, Figure S6).

5. Discussion

5.1. The Increase in Specific Discharge With Increasing Catchment Size Reflects the Increase in Contribution From Bedrock Groundwater

We demonstrated that specific discharge in the study catchments increased as the catchment area increased from 0.05 to 93.58 km² (Figure 4). Our analyses indicated that this increase in specific discharge was due to the mechanisms posited in Hypothesis (a); namely, a considerable portion of the precipitation in small headwater catchments infiltrates into bedrock and is discharged as surface water in larger downstream catchments. The spatial variation in precipitation levels posed in Hypothesis (b) had only small effects on this spatial pattern (Tables 2 and 3). This result was demonstrated in the small differences ($<13\%$) in precipitation among rain gauges and among catchments compared to differences in specific discharge of more

4.3. Comparison of Hydrographs

The log-log scatter plots of runoff at Locations Q, J, and D (Figure 5) clearly showed that specific discharge at the outlet of the smallest catchment, Location D (0.51 km²), was less than that at Locations Q (93.58 km²) and J (2.09 km²) throughout the observation period in 2014. Although the difference was small, the discharge was typically less for Location J than Location Q. A comparison of the hydrographs showed that the specific discharge of smaller catchments was less than that of larger catchments, even during periods of high flow (Figures 5 and S5).

The total discharge during the measurement period in 2014, when we had data from all three gauging stations (8 May to 24 October, 140 days; Figure S5), was 768, 588, and 171 mm for Locations Q, J, and D, respectively. Catchment mean normal annual precipitation levels based on mesh data were similar among locations, at 1,589, 1,525, and 1,585 mm for Q, J, and D, respectively (Table 2).

4.4. Temporal Patterns in Stable Isotopes

The LMWLs for the wet period ($\delta^2\text{H} = 7.8 \times \delta^{18}\text{O} + 10.4$, $r^2 = 0.92$, $p < 0.01$) and dry period ($\delta^2\text{H} = 6.9 \times \delta^{18}\text{O} + 1.4$, $r^2 = 0.92$,

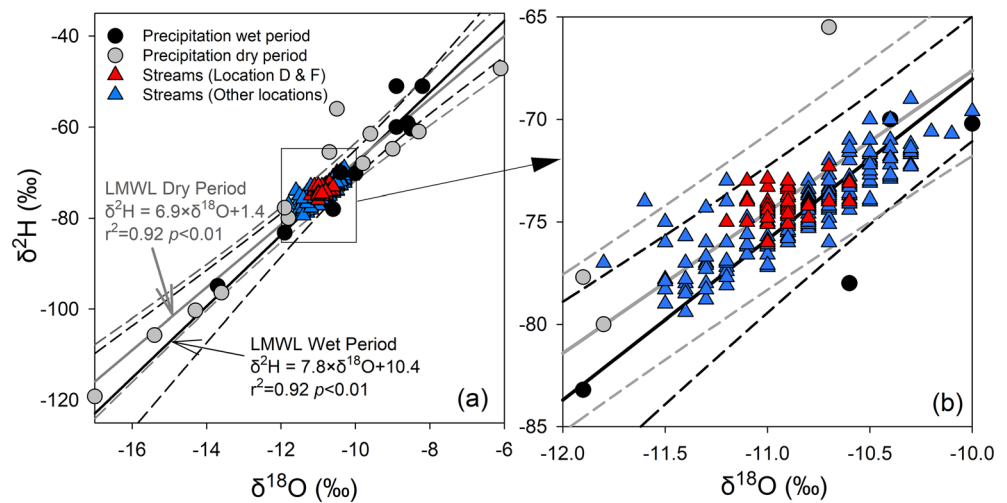


Figure 6. Plots of $\delta^{18}\text{O}$ versus $\delta^2\text{H}$ in precipitation during the wet (June–October) and dry (other months) periods and in stream water collected at Locations D and F (the nearest stream sampling locations to the P2 precipitation monitoring location) and other stream locations. Solid lines show the regression lines (LMWLs) for precipitation during the wet and dry periods, respectively. Broken lines show 95% confidence intervals for each regression line. A portion of (a) is enlarged in (b) for a detailed view.

than threefold under baseflow conditions and the lack of a significant relationship between catchment mean of 30-year normal annual precipitation and specific discharge (Tables 2 and 3). The hypothesized systematic changes in the separation of precipitation into quick flow and baseflow with catchment size in Hypothesis (c) did not appear to be the main factor determining the relationship between area and specific discharge during baseflow. Hydrographs from three locations showed that the smallest of the three catchments discharged less water per unit area, not only during baseflow but also during storm flow (Figure 5).

The data implied that small catchments leaked a considerable amount of water into the bedrock zone, with smaller catchments having less specific discharge (Figures 4 and 5). We conclude that this deep flow path contains mostly water transported in bedrock, as we observed fractured bedrock but little unconsolidated material or riparian area. Based on the difference between the specific discharge at continuous measurement sites D and J and at Q, we could roughly quantify the amount of leakage in small catchments. Assuming that the precipitation inputs and evapotranspiration outputs were similar among catchments and that the water budget was nearly closed at the largest location, Q, we measured only about 22% and 77% of the total water that the stream should carry at Locations D and J, respectively, during the measurement period. This result implies that a substantial amount of water left catchment D without passing the stream gauge at Location D. The observed phenomenon of water leakage in small catchments, and the return of this leaked groundwater to larger downstream catchments, has been demonstrated in other catchments (e.g., Egusa et al., 2016; Frisbee et al., 2011; Shaman et al., 2004), which supports the results of this study.

Our data did not show a clear threshold catchment size beyond which specific discharge did not increase any further (Figure 4). Specific discharge did not increase systematically with catchment size over about 30 km^2 (O, P, and Q) in any of the three campaigns (Table 2 and Figures 4d, 4f, and 4h), but the number of locations was limited and the data were scattered, and therefore more information is required to validate this threshold area. Some previous studies have identified a catchment area in which constant specific discharge is reached (Fujimoto et al., 2016; Shaman et al., 2004). The threshold areas in volcanic rock catchments reported by Fujimoto et al. (2016) coincided with the boundary between thick lava and pyroclastic flow deposition and a dissected channel that eroded headward, intersecting the flow paths of deep groundwater in the upper part of the catchment. Meanwhile, in the catchment of Devonian sedimentary rock and glacial till deposits investigated by Shaman et al. (2004), water infiltrated into bedrock through fractures and mostly discharged at the base of a steep slope. These observations imply that the threshold area may be related to subsurface structure and surface topography. This threshold area should be investigated further, as it is essential information for managing water resources and planning the gauging location. The annual water

Table 4
Means and Standard Deviations of $\delta^{18}\text{O}$ and $\delta^2\text{H}$ at Each Measurement Location

| Location ID | $\delta^{18}\text{O}$ (‰) | | $\delta^2\text{H}$ (‰) | | Number of samples |
|---------------------|---------------------------|--------------------|------------------------|--------------------|-------------------|
| | Mean | Standard deviation | Mean | Standard deviation | |
| A | -10.92 | 0.18 | -74.7 | 0.4 | 20 |
| B | -10.75 | 0.32 | -73.4 | 0.9 | 17 |
| C | -10.90 | 0.14 | -74.7 | 0.5 | 21 |
| D | -10.95 | 0.11 | -74.3 | 0.8 | 22 |
| E | -10.66 | 0.15 | -73.6 | 1.2 | 22 |
| F | -10.88 | 0.13 | -74.1 | 0.7 | 22 |
| G | -10.99 | 0.22 | -74.1 | 1.2 | 19 |
| H | -10.90 | 0.18 | -73.6 | 1.2 | 19 |
| I | -10.83 | 0.14 | -74.0 | 0.7 | 22 |
| J | -10.69 | 0.21 | -73.2 | 1.6 | 22 |
| K | -10.49 | 0.18 | -71.5 | 1.0 | 21 |
| L | -10.55 | 0.20 | -72.6 | 1.2 | 22 |
| M | -11.09 | 0.20 | -76.4 | 0.9 | 21 |
| N | -11.36 | 0.10 | -77.3 | 0.7 | 18 |
| O | -11.27 | 0.13 | -77.3 | 1.0 | 21 |
| P | -10.84 | 0.21 | -74.1 | 1.4 | 21 |
| Precipitation at P2 | -10.76 | 2.61 | -73.0 | 19.2 | 23 |

budget is often calculated to estimate evapotranspiration rates for an area (e.g., Brutsaert, 2005), and we intend to measure the water budget in catchments with areas above the threshold area.

5.2. Isotope Signals Correspond to Catchment Elevation

Isotopic enrichment due to kinetic isotope fractionation via evaporation in the subsurface flow path had only small effects on stream samples, as the isotopic composition of stream water generally aligned with the LMWL on the dual isotope plot (Figure 6). The large temporal fluctuations in the precipitation isotope signals nearly disappeared in streams (Table 4 and Figure S6), which demonstrates that precipitation isotope signals were dampened through mixing and dispersion in the subsurface flow path to the baseflow stream. This small temporal variation in stream isotope signals also supports the assumption that the sampled stream waters reflect the long-term mean isotope ratios of the precipitation feeding each stream.

The linear relationship between $\delta^{18}\text{O}$ and catchment mean elevation (Figure 7), which had a slope similar to the reported average isotopic lapse rate in central Japan, showed that the recharge elevation generally coincided with the mean elevation of the catchment. We drew lines based on reported isotopic lapse rates in central Japan (Yamanaka et al., 2015, 2016) for the largest sampling locations of Takikawa (Location P) and Irikawa (Location O) in Figure 7, as our

data indicated that smaller streams leaked considerable amounts of water. The lines for Locations P and O overlapped almost perfectly, and most stream samples fell near those lines, except a few divergent points, such as Locations A, H, and G (Figure 7).

The slight deviations of some plots, such as Locations A, H, and G, implies that in those catchments, a discrepancy existed between catchment mean elevation and mean recharge elevation. For example, the channel locations G and H were plotted above the line, as they had heavier $\delta^{18}\text{O}$ values than expected from mean elevation, which indicates that precipitation falling on the lower part of the catchment preferentially contributed to streams. Meanwhile, Location A was plotted below the line in Figure 7, as its $\delta^{18}\text{O}$ was lighter than expected from the mean elevation of the catchment, which indicates that precipitation falling at higher elevation preferentially contributed to stream. This indicates that leakage of water did not occur evenly over the entire area of those catchments. The data imply that the infiltration of water into bedrock may occur primarily through heterogeneously distributed fissures and joints in the bedrock.

Stable isotopes of water are a useful tracer in hydrological studies (e.g., Lutz et al., 2018; McGuire & McDonnell, 2006). However, our study site was subjected to monthly sampling of precipitation and stream water over 2 years, and large fluctuations observed in precipitation were quite diminished in stream water samples. Analyses such as transit time estimation require that the seasonal isotope signal in precipitation be reflected in the isotope signals of stream water, but our streamflow data did not show that relationship (Figure S6). Furthermore, the studied elevation range may have been insufficient. With a maximum difference in mean elevation of 497 m, the differences in mean isotope ratios among locations were relatively small compared to temporal fluctuations, which were minor but present (Figure 7). For this reason, further quantitative analyses using this stable isotope data would be difficult.

5.3. Scatter in the Relationship Between Catchment Area and Specific Discharge

There was relatively large scatter in the data, although an overall increase in specific discharge with increasing catchment area was apparent (Figure 4). The deviations in the smallest location, A, and other small (<0.05 km²) catchments in our preliminary measurements (Asano et al., 2013) showed large variability among small catchments, similar to the results of previous studies, which decreased with increasing catchment area of about 1 km² (e.g., Woods et al., 1995). In addition, our data showed variability in areas greater than 1 km², such as Locations K (2.2 km²) and L (2.9 km²; Table 2). This trend of decreasing variability with area may depend on the mechanism driving the variability. However, we have insufficient data to analyze

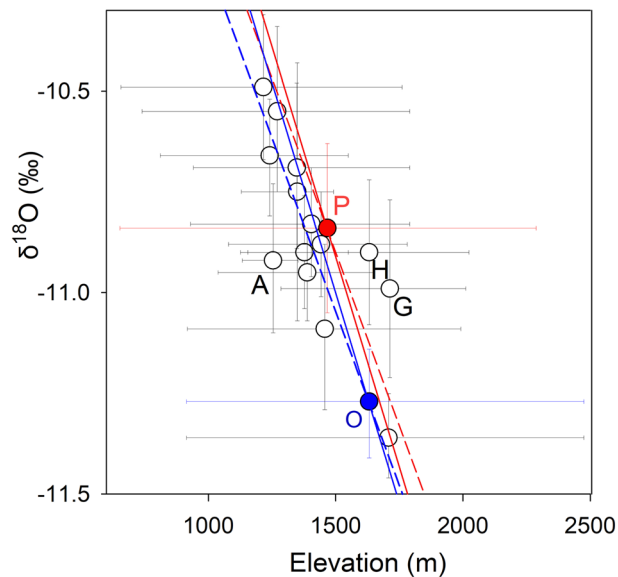


Figure 7. Relationships between mean elevations of catchment and mean $\delta^{18}\text{O}$ of streams at each catchment. Horizontal bars indicate the maximum and minimum elevations of each catchment, and vertical bars indicate the standard deviations of $\delta^{18}\text{O}$ values. Solid lines show reported arithmetic average isotopic lapse rates for central Japan (-2.086‰ km^{-1} ; Yamanaka et al., 2016), and broken lines show lapse rates based on multiple regression analyses for central Japan (-1.724‰ km^{-1} ; Yamanaka et al., 2015) for the largest measured locations in Takikawa (Location P) in red and Irikawa (Location O) in blue color.

the cause of the variability in this study, and therefore we only list several possible sources of scatter in our data. Some of the scatter in our data may be attributable to heterogeneous bedrock flow paths, which is supported by the isotope signals (e.g., A, H, and G in Figure 7). Evapotranspiration and soil depth can exhibit spatial variability and can affect low-flow discharge (e.g., Lyon et al., 2012), in particular in our steep catchment with a montane to subalpine vegetation zone. Although the effects would be small in a steep mountain stream, hyporheic flow can reduce instantaneous flow measurements in natural gravel or boulder bed rivers (Payn et al., 2012).

5.4. Catchments in Which Specific Discharge Increased With Catchment Size

We summarized previously reported data for the area-specific discharge relationship, focusing on the average catchment slope, geology, quaternary deposits, and hydraulic properties of the bedrock to determine which catchment conditions controlled the spatial pattern in flow (Table 5). Those properties were selected because previous studies have demonstrated that the hydraulic properties of bedrock and distribution of unconsolidated sediment control the contribution of deep groundwater to low flow-specific discharge (e.g., Hale & McDonnell, 2016; Komatsu & Onda, 1996; Onda et al., 2006) and that catchment topographic factors, such as the mean slope angle, can increase the amount of bedrock storage from studies of mesoscale catchment (e.g., Sayama et al., 2011).

The catchments that followed the pattern of increasing specific discharge with area were described as consisting of “permeable bedrock” (Table 5), which implies that in catchments in which specific discharge increased with area, bedrock contributed to storage and discharge in mesoscale subcatchments. Six reported catchments that showed increasing specific discharge with catchment area were underlain by sedimentary rock and volcanic rock. In general, those catchments were steep (5–67%). Meanwhile, some sedimentary rock and volcanic rock catchments also exhibited independent and decreasing specific discharge with area, and some steep catchments had independent and decreasing specific discharge with area. This shows that more details beyond commonly available bedrock type and slope might be necessary to point out the catchment with the potential for bedrock storage being important to stream flow.

5.5. Catchment Area and Baseflow-Specific Discharge Relationships May Qualitatively Describe the Contribution and Depth of Deep Flow Paths

Previous studies that demonstrated decreasing specific discharge with catchment area (Figure 1c, Table 5) implied that more water is stored in bedrock fractures and quaternary deposits in smaller catchments compared to larger catchments, and thus smaller catchments contribute disproportionately to low flows. They also indicated that the infiltration of streamflow into the streambed in larger catchments can result in the observed decreasing pattern (Florincic et al., 2019; Tetzlaff & Soulsby, 2008). A study in one catchment with a constant baseflow-specific discharge relationship reported that the average contribution of bedrock flow was similar for both small and large streams, with contributions of bedrock groundwater ranging between 42% to 62% for third- to sixth-order streams under baseflow conditions (Uchida & Asano, 2010). This implies that for a catchment with an independent baseflow-specific discharge relationship, the bedrock flow and flow from deposits may contribute almost equally, independent of catchment size, or these flows may contribute very little, independent of catchment size. Other studies that have compared stream baseflow among streams that are not nested have also demonstrated that the spatial distribution of stream baseflow can reflect the subsurface hydrologic structure (Payn et al., 2012; Price et al., 2011; Sun et al., 2017; Zimmer & Gannon, 2018). Those studies support the area-specific discharge relationship as a useful tool for assessing the storage and discharge properties of a catchment, although more information on the processes behind each spatial pattern is still needed.

Table 5
Reported Relationships Between Area and Specific Discharge During Baseflow or Low-Flow Conditions Based on Field Measurements With a Nested Design

| Reference | Study sites | Area-specific dis. relationship | Increasing (decreasing) until catchment areas of (km ²) | Increasing (decreasing) trend start at (km ²) | Number of observation points | Maximum observed catchment area (km ²) | Minimum observed area (km ²) | Average slope (%) | Bedrock type |
|--|---------------------------------------|---------------------------------|---|---|------------------------------|--|--|-------------------|----------------------|
| This study | Irikawa and Takikawa, Saitama, Japan | Increasing | - | 0.1 | 13 | 93.58 | 0.05 | 67 | Sedimentary |
| Egusa et al. (2016) | Inokawa catchment, Chiba, Japan | Increasing | >5 ^a | 1 ^a | 113 | 5.07 | 0.012 | 60 ± 24 | Sedimentary |
| Fujimoto et al. (2016) | Mt. Daisen, Tottori, Japan | Increasing | 2–3 | 0.3 | 48 | 10.6 | <0.3 | 15 ^d | Volcanic |
| Floriancic et al. (2019) | P1, P4, and V2 catchment, Swiss | Increasing | - | - | 6–9 | 19.5 | 0.2 | 15–47 | Sedimentary |
| Shaman et al. (2004), Shaw et al. (2017) | Catskill Mountains, NY, USA | Increasing | 8–21 | - | 11 | 176 | 1.64 | 5 ^d | Sedimentary |
| Tague and Grant(2004) | Cascade streams, OR, USA | Increasing ^{a,b,c,d} | - | - | 27 | 3,463 | 19.0 | - | Volcanic |
| Asano et al. (2009) | Fudoji, Shiga, Japan | Independent | - | - | 76 | 4.27 | 0.00018 | 10 ^d | Plutonic |
| Woods et al. (1995) | Little Akaola, New Zealand | Independent | - | - | 28 | 14.08 | 4.87 | 2 | Volcanic |
| Woods et al. (1995) | Lewis River, New Zealand | Independent | - | - | 24 | 52.4 | 4.4 | 4 (2.7–10) | Sedimentary |
| Egusa et al. (2013) | Yozukugawa catchment, Kanagawa, Japan | Independent | - | - | 65 | 55.6 | 0.013 | 61 | Plutonic |
| Lyon et al. (2012) | Krycklan catchment, Sweden | Independent | - | - | 80 | 67 | 0.12 | 2–7 | Sedimentary |
| Floriancic et al. (2019) | 9 measured catchments, Swiss | Decreasing | - | - | 5–13 | 109.1 | 0.1 | 13–63 | Sedimentary/others |
| Tetzlaff and Soulsby (2008) | River Dee, Scotland, UK | Decreasing ^{a,c,d} | 1,849 ^a | 500 ^a | 22 | 1,849 | 11.1 | 13 (3–25) | Plutonic/sedimentary |

Note. “-” indicate that no information can be found.

^aTrend in area-specific discharge relationships and catchment areas of increasing/decreasing trend were read from literature by authors. ^bMean August flow. ^cMean annual flow. ^dSlope of the catchment was calculated dividing altitude difference between highest and lowest points in catchment by distance between these two points based on topographic map.

Table 5
Continued

| Reference | Age | Other strata description | Available information on bedrock property |
|--|-------------------------|--|--|
| This study | Cretaceous | Mesozoic accretionary complex | Many faults and joints exist (Chichibu Geologic Research Group, 1966; Hara et al., 2010) |
| Egusa et al. (2016) | Tertiary | Neogene sedimentary rock | Oda et al., 2008 measured 520 mm/yr (22% of the annual precipitation) infiltrated into the bedrock and runs off without passing through a weir gauge (0.012 km ²). Young lavas are extremely permeable (Saar & Manga, 2004) |
| Fujimoto et al. (2016) | Quaternary | Located around the Karasugasen lava dome, erupted at approximately 26 ka. Pyroclastic flow deposits, some of which were more than 100 m thick. | Young lavas are extremely permeable (Saar & Manga, 2004) |
| Floriancic et al. (2019) | - | Quaternary deposit covers 55–66% of catchment | The sandstone molasse layers appears to be a storage element that contributes more to low flow. |
| Shaman et al. (2004), Shaw et al. (2017) | Devonian | The bedrock is primarily coarse sandstone and conglomerate with interbedded shale and siltstone (Way, 1972). Glacial till overlies the bedrock throughout much of the watershed and colluvium and alluvium are present in riparian areas (Rich, 1934). | Most of the beds are cut by three nearly perpendicular sets of fractures, one of which is parallel to the bedding plane ... increases the permeability of the bedrock, and results in groundwater springs at the base of steep slopes. Discharge from bedrock plays important roles in maintaining low flow in headwater stream (Burns et al., 1998) |
| Tague and Grant (2004) | Miocene and Pleistocene | Rivers generally flow perpendicular to the strike of two distinct geologic provinces; the Western and High Cascades. Summer streamflow volumes, recession characteristics, and timing of response to winter recharge are all linearly related to the percent of High Cascade geology in the contributing area. | The Western Cascade: Typically well drained, with soils 1–3 m in depth of moderate to high surface hydraulic conductivities grading vertically to shallow subsurface confining layers of clay, saprolite and unweathered bedrock of generally low permeability. The High Cascade: surface and subsurface hydraulic conductivities in young volcanic deposits are exceptionally high due to highly porous and permeable volcanic layers. |
| Asano et al. (2009) | Cretaceous | Granite. The bedrock is weathered and fractured. | For the granite in this region, Katsura et al. (2009) showed that bedrock is moderately to highly weathered and core scale K_s value range 10^{-5} to 10^{-3} cm/s. The similarity of the in situ K_s to core-scale suggested water flow could be characterized as matrix flow. |
| Woods et al. (1995) | - | Valley dissects andesitic and basaltic lava flows and tephra deposits, lower slopes overlain by loss. | - |
| Woods et al. (1995) | - | Strongly indurated greywacke and argillite | - |
| Egusa et al. (2013) | Tertiary | Granodiorite and volcanic rocks of Miocene | - |
| Lyon et al. (2012) | Proterozoic | Svecofennian rocks with 94% metasediments/metagraywacke deposited with glacial till, peat and mires (Ågren et al., 2007). | - |
| Floriancic et al. (2019) | - | Quaternary deposit covers 49–67% of catchment. Significant infiltration of streamflow into the streambed. In the Alpine catchments, larger and thicker quaternary sediment layers (particularly glacial and alluvial deposits) might favor percolation to deeper groundwater stores and therefore results in higher low flows. | Headwater catchment disproportionately contribute to low flows. Relatively large proportion of discharge during low flow comes from landforms that are less common in larger catchment. |
| Tetzlaff and Soulsby (2008) | Precambrian | The solid geology is overlain by a range of drift deposits of varying thickness reflecting the complex glacial history. Alluvium and fluvio-glacial deposits fill the bottom of much of the main river valleys and glacial till covers the lower slopes of many valley sides. Many of the drifts have significant water storage potential and can be important sources of groundwater. | Although these units are usually considered as aquitards with very low primary porosity, fractures in the upper 10 m or so of the granites can be important groundwater flow paths (Soulsby et al., 1998). Although fractures in the schists also occur, the intensity of these is usually lower (Soulsby et al., 2005). The upper 54% of the catchment contributed 71% of baseflow in the lower river, indicative that sufficient groundwater is stored in the various drifts and bedrock fracture. |

Note. “-” indicate that no information can be found.

^aTrend in area-specific discharge relationships and catchment areas of increasing/decreasing trend were read from literature by authors. ^bMean August flow.

^cMean annual flow. ^dSlope of the catchment was calculated dividing altitude difference between highest and lowest points in catchment by distance between these two points based on topographic map.

The analyses conducted herein imply that the effects of flow paths in bedrock as a dominant storage reservoir for water can be assessed by measuring the relationship between topographic catchment area and specific discharge during baseflow. Meanwhile, the area-specific discharge relationship provides qualitative information on the storage properties of mesoscale steep catchments, and quantitative assessment should now be conducted. For example, this study qualitatively shows that the catchments have deep bedrock storage, which should contribute to flow only in larger catchments. Meanwhile, studies of the hydraulic properties of catchments in relation to bedrock geology in Japan have shown that baseflow is largest for quaternary volcanic rock and declines in the order of granitic rock, tertiary volcanic rock, and Mesozoic and Paleozoic sedimentary rock (Musiak et al., 1981). This implies that a catchment underlain with Mesozoic and Paleozoic sedimentary rock is characterized by less groundwater storage than other rock types in Japanese archipelago, although the depth of bedrock storage appears greater in our study. We still have limited information regarding the properties and functions of bedrock storage, and further quantification of the amount and clarifying the function of storage is needed for the effective water resources management.

6. Conclusions

In the Irikawa and Takikawa catchments in the headwaters of the Arakawa River, specific discharge increased more than threefold with catchment area over the range of 0.05 to 93.58 km². Analyses of the spatial variation in precipitation, hydrographs from three gauged locations, and isotopic signals supported Hypothesis (a), which states that a considerable amount of precipitation that infiltrates the bedrock in hillslopes does not return to surface flow at the outlet of a small catchment but instead is discharged in larger catchments downstream. Meanwhile, our other hypotheses, namely, (b) spatial patterns in precipitation and (c) spatial variation in the partitioning of storm flow and baseflow, did not reflect the major causes of increasing specific discharge with catchment area. The data for catchment areas greater than 20 km² were limited, and these data were scattered, and therefore the threshold catchment area in which most of the residuals of precipitation falling upstream minus evapotranspiration discharged through local streams and specific discharge did not increase further was unclear based on our results. Further assessment is required when more data become available for larger drainage areas.

This study and previous studies demonstrate that the storage of water in mesoscale catchments is strongly related to subsurface structure, such as the distribution and depth of permeable bedrock. However, such structure is often difficult to assess based on easily available information such as surface topography and geology. This study provides a basis for determining the storage-discharge properties of a mesoscale mountain catchment based on a simple area-specific discharge relationship. More information is still needed, regarding the processes behind each spatial pattern and a method for quantitatively assessing the storage and discharge properties of mesoscale catchments.

Data Availability Statement

We thank Ministry of Land, Infrastructure, Transport and Tourism, Kanto Regional Development Bureau, Futase Dam office for providing the discharge data. The data can be available for download (<http://doi.org/10.15083/00078601>).

Acknowledgments

This study was funded by a research grant from the joint project between the University of Tokyo Chichibu Forest and Suntory Natural Water Sanctuary and JSPS KAKENHI Grant JP18K05741. We thank members of The University of Tokyo Chichibu Forest for water sampling, management of discharge weirs, and access to the sites. We thank anonymous reviewers for valuable comments. Discharge data were provided by the Ministry of Land, Infrastructure, Transport and Tourism and by Tokyo Electric Power Company Holdings.

References

- Ågren, A., Buffam, I., Jansson, M., & Laudon, H. (2007). Importance of seasonality and small streams for the landscape regulation of dissolved organic carbon export. *Journal of Geophysical Research*, *112*, G03003. <https://doi.org/10.1029/2006JG000381>
- Anderson, S. P., Dietrich, W. E., Montgomery, D. R., Topp, R., Conrad, M. E., & Loague, K. (1997). Subsurface flow paths in a steep, unchanneled catchment. *Water Resources Research*, *33*(12), 2637–2653. <https://doi.org/10.1029/97WR02595>
- Asano, Y., Saito, T., Kimura, K., Haraguchi, R., & Chishima, T. (2017). Discharge measurement using an erosion control dam at Yatakezawa in the University of Tokyo Chichibu Forest—Water height and discharge relationships of lower level notch at the multiple dimensional spillway of the secondary dam. *Miscellaneous Information, the University of Tokyo Forests*, *59*, 235–243. <https://doi.org/10.15083/00026124> (in Japanese)
- Asano, Y., Kawasaki, M., Fujiwara, N., Ohmura, K., Takano, M., Chishima, T., et al. (2013). Preliminary investigation for location of stream chemistry monitoring in Irikawa catchment at The University of Tokyo Chichibu Forest. *Miscellaneous Information, the University of Tokyo Forests*, *53*, 153–167. <https://doi.org/10.15083/00026167> (in Japanese)
- Asano, Y., & Uchida, T. (2010). Is representative elementary area defined by a simple mixing of variable small streams in headwater catchments? *Hydrological Processes*, *24*(5), 666–671. <https://doi.org/10.1002/hyp.7589>

- Asano, Y., Uchida, T., Gomi, T., Mizugaki, S., Hiraoka, M., Katsuyama, M., et al. (2018). Effects of spatial scales on runoff/sediment transport in mountain catchments (1)—A review of field observations on catchment area and properties. *Journal of Japan Society of Hydrology and Water Resources*, 31(4), 219–231. <https://doi.org/10.3178/jjshwr.31.219> (in Japanese with English abstract)
- Asano, Y., Uchida, T., Mimasu, Y., & Ohte, N. (2009). Spatial patterns of stream solute concentrations in a steep mountainous catchment with a homogeneous landscape. *Water Resources Research*, 45, W10432. <https://doi.org/10.1029/2008WR007466>
- Blöschl, G., & Sivapalan, M. (1997). Process controls on regional flood frequency: Coefficient of variation and basin scale. *Water Resources Research*, 33(12), 2967–2980. <https://doi.org/10.1029/97WR00568>
- Brutsaert, W. (2005). *Hydrology: An introduction* (p. 618). New York, NY: Cambridge University Press. <https://doi.org/10.1017/CBO9780511808470>
- Burns, D. A., Murdoch, P. S., & Lawrence, G. B. (1998). Effect of groundwater springs on NO₃⁻ concentrations during summer in Catskill Mountain streams. *Water Resources Research*, 34(8), 1987–1996. <https://doi.org/10.1029/98WR01282>
- Chichibu Geologic Research Group (1966). Geology in the vicinity of the Tokyo University Forest at Chichibu. *Miscellaneous Information, the University of Tokyo Forests*, 16, 73–85. <https://doi.org/10.15083/00026363> (in Japanese with English abstract)
- Clark, I., & Fritz, P. (1997). *Environmental isotopes in hydrogeology* (p. 328). New York, NY: CRC Press.
- Craig, H. (1961). Isotopic variations in meteoric waters. *Science*, 133(3465), 1702–1703. <https://doi.org/10.1126/science.133.3465.1702>
- Dansgaard, W. (1964). Stable isotopes in precipitation. *Tellus*, 16(4), 436–468. <https://doi.org/10.1111/j.2153-3490.1964.tb00181.x>
- Didszun, J., & Uhlenbrook, S. (2008). Scaling of dominant runoff generation processes: Nested catchments approach using multiple tracers. *Water Resources Research*, 44, W02410. <https://doi.org/10.1029/2006WR005242>
- Egusa, T., Kumagai, T., Oda, T., Gomi, T., & Ohte, N. (2019). Contrasting patterns in the decrease of spatial variability with increasing catchment area between stream discharge and water chemistry. *Water Resources Research*, 55, 7419–7435. <https://doi.org/10.1029/2018WR024302>
- Egusa, T., Ohte, N., Oda, T., & Suzuki, M. (2013). Relationship between catchment scale and the spatial variability of stream discharge and chemistry in a catchment with multiple geologies. *Hydrological Research Letters*, 7(2), 12–17. <https://doi.org/10.3178/hrl.7.12>
- Egusa, T., Ohte, N., Oda, T., & Suzuki, M. (2016). Quantifying aggregation and change in runoff source in accordance with catchment area increase in a forested headwater catchment. *Hydrological Processes*, 30(22), 4125–4138. <https://doi.org/10.1002/hyp.10916>
- Floriancic, M. G., Fischer, B. M. C., Molnar, P., Kirchner, J. W., & Meerveld, I. H. J. (2019). Spatial variability in specific discharge and streamwater chemistry during low flows: Results from snapshot sampling campaigns in eleven Swiss catchments. *Hydrological Processes*, 33(22), 2847–2866. <https://doi.org/10.1002/hyp.13532>
- Frisbee, M. D., Phillips, F. M., Campbell, A. R., Liu, F., & Sanchez, S. A. (2011). Streamflow generation in a large, alpine watershed in the southern Rocky Mountains of Colorado: Is streamflow generation simply the aggregation of hillslope runoff responses? *Water Resources Research*, 47, W06512. <https://doi.org/10.1029/2010WR009391>
- Fujimoto, M., Ohte, N., Kawasaki, M., Osaka, K., Itoh, M., Ohtsuka, I., & Itoh, M. (2016). Influence of bedrock groundwater on streamflow characteristics in a volcanic catchment. *Hydrological Processes*, 30(4), 558–572. <https://doi.org/10.1002/hyp.10558>
- Furey, P. R., & Gupta, V. K. (2005). Effects of excess rainfall on the temporal variability of observed peak-discharge power laws. *Advances in Water Resources*, 28(11), 1240–1253. <https://doi.org/10.1016/j.advwatres.2005.03.014>
- Gomi, T., Sidle, R. C., & Richardson, J. S. (2002). Understanding processes and downstream linkages of headwater systems: Headwaters differ from downstream reaches by their close coupling to hillslope processes, more temporal and spatial variation, and their need for different means of protection from land use. *Bioscience*, 52(10), 905–916. [https://doi.org/10.1641/0006-3568\(2002\)052\[0905:upad\]2.0.co;2](https://doi.org/10.1641/0006-3568(2002)052[0905:upad]2.0.co;2)
- Hale, V. C., & McDonnell, J. J. (2016). Effect of bedrock permeability on stream base flow mean transit time scaling relations: 1. A multiscale catchment intercomparison. *Water Resources Research*, 52, 1358–1374. <https://doi.org/10.1002/2014WR016124>
- Hara, H., Ueno, H., Tsunoda, K., Hisada, K., Shimizu, M., Takeuchi, K., & Ozaki, M. (2010). *Geology of the Mitsumine District. Quadrangle Series, 1: 50,000*, Geological Survey of Japan, AIST, 110 p. (in Japanese with English abstract 4 p.)
- Japan Meteorological Agency (1981–2010). *30-year normal precipitation data*. Retrieved from <https://www.data.jma.go.jp/obd/stats/etrn/view/atlas.html>
- Katsura, S., Kosugi, K., Mizutani, T., & Mizuyama, T. (2009). Hydraulic properties of variously weathered granitic bedrock in headwater catchments. *Vadose Zone Journal*, 8(3), 557–573. <https://doi.org/10.2136/vzj2008.0142>
- Katsuyama, M., Tani, M., & Nishimoto, S. (2010). Connection between streamwater mean residence time and bedrock groundwater recharge/discharge dynamics in weathered granite catchments. *Hydrological Processes*, 24(16), 2287–2299. <https://doi.org/10.1002/hyp.7741>
- Kimura, K., Saito, T., Aikawa, M., Igarashi, Y., Chishima, T., & Asano, Y. (2015). Discharge measurement at Bakemono-sawa in the University of Tokyo Chichibu Forest. *Miscellaneous Information of The University of Tokyo Forests*, 57, 61–73. <https://doi.org/10.15083/00026136>
- Kohler, M. A., & Linsley, R. K. Jr. (1951). *Predicting runoff from storm rainfall, Research Paper 34*. Washington DC: US Weather Bureau.
- Komatsu, Y., & Onda, Y. (1996). Spatial variation in specific discharge of base flow in a small catchments, Oe-yama region, Western Japan. *Journal of Japan Society of Hydrology and Water Resources*, 9(6), 489–497. <https://doi.org/10.3178/jjshwr.9.489>
- Kondo, J., Nakazono, M., Watanabe, T., & Kuwagata, T. (1992). Hydrological climate in Japan (3)—Evapotranspiration from forest. *Journal of Japan Society of Hydrology and Water Resources*, 5(4), 8–18. https://doi.org/10.3178/jjshwr.5.4_8 (in Japanese with English abstract)
- Kosugi, K., Katsura, S., Mizuyama, T., Okunaka, S., & Mizutani, T. (2008). Anomalous behavior of soil mantle groundwater demonstrates the major effects of bedrock groundwater on surface hydrological processes. *Water Resources Research*, 44, W01407. <https://doi.org/10.1029/2006WR005859>
- Laudon, H., & Sponseller, R. A. (2018). How landscape organization and scale shape catchment hydrology and biogeochemistry: Insights from a long-term catchment study. *WIREs Water*, 5(2), e1265. <https://doi.org/10.1002/wat2.1265>
- Liebming, A., Haberhauer, G., Papesch, W., & Heiss, G. (2006). Correlation of the isotopic composition in precipitation with local conditions in alpine regions. *Journal of Geophysical Research*, 111, D05104. <https://doi.org/10.1029/2005JD006258>
- Lutz, S. R., Krieg, R., Müller, C., Zink, M., Knöller, K., Samaniego, L., & Merz, R. (2018). Spatial patterns of water age: Using young water fractions to improve the characterization of transit times in contrasting catchments. *Water Resources Research*, 54, 4767–4784. <https://doi.org/10.1029/2017WR022216>
- Lyon, S. W., Nathanson, M., Spans, A., Grabs, T., Laudon, H., Temnerud, J., et al. (2012). Specific discharge variability in a boreal landscape. *Water Resources Research*, 48, W08506. <https://doi.org/10.1029/2011WR011073>
- McGuire, K. J., & McDonnell, J. J. (2006). A review and evaluation of catchment transit time modeling. *Journal of Hydrology*, 330(3-4), 543–563. <https://doi.org/10.1016/j.jhydrol.2006.04.020>

- Meteorology Division, Fundamental data Development Committee, The University of Tokyo Forests (2018). Annual report of meteorological observations in the University of Tokyo Forest, The University of Tokyo (Jan. 2016 – Dec 2016). *Miscellaneous Information, the University of Tokyo Forests*, 60, 101–120. <https://doi.org/10.15083/00074143> (in Japanese)
- Ministry of Land Infrastructure, and Transport and Tourism of Japan, Water Information System (n.d.), <http://www1.river.go.jp/>
- Montgomery, D. R., & Buffington, J. M. (1997). Channel-reach morphology in mountain drainage basins. *Geological Society of America Bulletin*, 109(5), 596–611. [https://doi.org/10.1130/0016-7606\(1997\)109<0596:crmimd>2.3.co;2](https://doi.org/10.1130/0016-7606(1997)109<0596:crmimd>2.3.co;2)
- Musiake, K., Takahasi, Y., & Ando, Y. (1981). Effects of basin geology on river-flow regime in mountainous areas of Japan. *Proceedings. Japan Society of Civil Engineers*, 1981(309), 51–62. https://doi.org/10.2208/jscej1969.1981.309_51 (in Japanese)
- Oda, T., Asano, Y., & Suzuki, M. (2008). Estimating deep percolation in a small catchment in a tertiary formation using the chloride mass balance method. *Journal of Japan Society of Hydrology and Water Resources*, 21(3), 195–204. <https://doi.org/10.3178/jjshwr.21.195>. (in Japanese with English summary)
- Ogden, F., & Dawdy, D. (2003). Peak discharge scaling in small Hortonian watershed. *Journal of Hydrologic Engineering*, 8(2), 64–73. [https://doi.org/10.1061/\(ASCE\)1084-0699\(2003\)8:2\(64\)](https://doi.org/10.1061/(ASCE)1084-0699(2003)8:2(64))
- Onda, Y., Komatsu, Y., Tsujimura, M., & Fujihara, J. (2001). The role of subsurface runoff through bedrock on stream flow generation. *Hydrological Processes*, 15(10), 1693–1706. <https://doi.org/10.1002/hyp.234>
- Onda, Y., Tsujimura, M., Fujihara, J.-I., & Ito, J. (2006). Runoff generation mechanisms in high-relief mountainous watersheds with different underlying geology. *Journal of Hydrology*, 331(3–4), 659–673. <https://doi.org/10.1016/j.jhydrol.2006.06.009>
- Payn, R. A., Gooseff, M. N., McGlynn, B. L., Bencala, K. E., & Wondzell, S. M. (2012). Exploring changes in the spatial distribution of stream baseflow generation during a seasonal recession. *Water Resources Research*, 48(4), W04519. <https://doi.org/10.1029/2011WR011552>
- Peralta-Tapia, A., Sponseller, R. A., Ågren, A., Tetzlaff, D., Soulsby, C., & Laudon, H. (2015). Scale-dependent groundwater contributions influence patterns of winter baseflow stream chemistry in boreal catchments. *Journal of Geophysical Research: Biogeosciences*, 120, 847–858. <https://doi.org/10.1002/2014JG002878>
- Peters, E., Visser, A., Esser, B., & Moran, J. (2018). Tracers reveal recharge elevations, groundwater flow paths and travel times on Mount Shasta, California. *Water*, 10(2), 97. <https://doi.org/10.3390/w10020097>
- Pfister, L., Martínez-Carreras, N., Hissler, C., Klaus, J., Carrer, G. E., Stewart, M. K., & McDonnell, J. J. (2017). Bedrock geology controls on catchment storage, mixing, and release: A comparative analysis of 16 nested catchments. *Hydrological Processes*, 31(10), 1828–1845. <https://doi.org/10.1002/hyp.11134>
- Price, K., Jackson, C. R., Parker, A. J., Reitan, T., Dowd, J., & Cyterski, M. (2011). Effects of watershed land use and geomorphology on stream low flows during severe drought conditions in the southern Blue Ridge Mountains, Georgia and North Carolina, United States. *Water Resources Research*, 47, W02516. <https://doi.org/10.1029/2010WR009340>
- Rich, J. L. (1934). *Glacial geology of the Catskill Mountains* (Vol. 29, p. 180). New York: State Museum Bulletin.
- Roy, J. W., & Hayashi, M. (2009). Multiple, distinct groundwater flow systems of a single moraine-talus feature in an alpine watershed. *Journal of Hydrology*, 373(1–2), 139–150. <https://doi.org/10.1016/j.jhydrol.2009.04.018>
- Saar, M. O., & Manga, M. (2004). Depth dependence of permeability in the Oregon Cascades inferred from hydrogeologic, thermal, seismic, and magmatic modeling constraints. *Journal of Geophysical Research*, 109, B04204. <https://doi.org/10.1029/2003JB002855>
- Saitama Prefecture (1987). Arakawa: Arakawa General Survey Report, Saitama Prefecture, <https://doi.org/10.11501/9644097>
- Sawano, S., Hotta, N., Tanaka, N., Tsuboyama, Y., & Suzuki, M. (2015). Development of a simple forest evapotranspiration model using a process-oriented model as a reference to parameterize data from a wide range of environmental conditions. *Ecological Modelling*, 309–310, 93–109. <https://doi.org/10.1016/j.ecolmodel.2015.04.011>
- Sayama, T., McDonnell, J. J., Dhakal, A., & Sullivan, K. (2011). How much water can a watershed store? *Hydrological Processes*, 25(25), 3899–3908. <https://doi.org/10.1002/hyp.8288>
- Shaman, J., Stieglitz, M., & Burns, D. (2004). Are big basins just the sum of small catchments? *Hydrological Processes*, 18(16), 3195–3206. <https://doi.org/10.1002/hyp.5739>
- Shaw, S. B., Bonville, D. B., & Chandler, D. G. (2017). Combining observations of channel network contraction and spatial discharge variation to inform spatial controls on baseflow in Birch Creek, Catskill Mountains, USA. *Journal of hydrology: Regional studies*, 12, 1–12. <https://doi.org/10.1016/j.ejrh.2017.03.003>
- Singh, V. P. (1997). Effect of spatial and temporal variability in rainfall and watershed characteristics on stream flow hydrograph. *Hydrological Processes*, 11(12), 1649–1669. [https://doi.org/10.1002/\(SICI\)1099-1085\(19971015\)11:12<1649::AID-HYP495>3.0.CO;2-1](https://doi.org/10.1002/(SICI)1099-1085(19971015)11:12<1649::AID-HYP495>3.0.CO;2-1)
- Soulsby, C., Chen, M., Ferrier, R. C., Jenkins, A., & Harriman, R. (1998). Hydrogeochemistry of shallow groundwater in a Scottish catchment. *Hydrological Processes*, 12(7), 1111–1127. [https://doi.org/10.1002/\(SICI\)1099-1085\(19980615\)12:7<1111::AID-HYP633>3.0.CO;2-2](https://doi.org/10.1002/(SICI)1099-1085(19980615)12:7<1111::AID-HYP633>3.0.CO;2-2)
- Soulsby, C., Malcolm, I. A., Youngson, A. F., Tetzlaff, D., Gibbins, C. N., & Hannah, D. M. (2005). Groundwater–surface water interactions in upland Scottish rivers: hydrological, hydrochemical and ecological implications. *Scottish Journal of Geology*, 41(1), 39–49.
- Soulsby, C., Tetzlaff, D., & Hrachowitz, M. (2009). Tracers and transit times: Windows for viewing catchment scale storage? *Hydrological Processes*, 23(24), 3503–3507. <https://doi.org/10.1002/hyp.7501>
- Strahler, A. N. (1952). Hypsometric (area-altitude) analysis of erosional topography. *Geological Society of America Bulletin*, 63(11), 1117–1142. [https://doi.org/10.1130/0016-7606\(1952\)63](https://doi.org/10.1130/0016-7606(1952)63)
- Sun, H., Kasahara, T., Otsuki, K., Saito, T., & Onda, Y. (2017). Spatio-temporal streamflow generation in a small, steep headwater catchment in western Japan. *Hydrological Sciences Journal*, 62(5), 818–829. <https://doi.org/10.1080/02626667.2016.1266635>
- Tague, C., & Grant, G. E. (2004). A geological framework for interpreting the low-flow regimes of Cascade streams, Willamette River Basin, Oregon. *Water Resources Research*, 40, W04303. <https://doi.org/10.1029/2003WR002629>
- Temnerud, J., Seibert, J., Jansson, M., & Bishop, K. (2007). Spatial variation in discharge and concentrations of organic carbon in a catchment network of boreal streams in northern Sweden. *Journal of Hydrology*, 342(1–2), 72–87. <https://doi.org/10.1016/j.jhydrol.2007.05.015>
- Tetzlaff, D., & Soulsby, C. (2008). Sources of baseflow in larger catchments—Using tracers to develop a holistic understanding of runoff generation. *Journal of Hydrology*, 359(3–4), 287–302. <https://doi.org/10.1016/j.jhydrol.2008.07.008>
- Tóth, J. (1963). A theoretical analysis of groundwater flow in small drainage basins. *Journal of Geophysical Research*, 68(16), 4795–4812. <https://doi.org/10.1029/JZ068i016p04795>
- Tromp-van Meerveld, H. J., & McDonnell, J. J. (2006). Threshold relations in subsurface stormflow: 2. The fill and spill hypothesis. *Water Resources Research*, 42, W02411. <https://doi.org/10.1029/2004WR003800>
- Tsuboyama, Y., Sidle, R. C., Noguchi, S., & Hosoda, I. (1994). Flow and solute transport through the soil matrix and macropores of a hillslope segment. *Water Resources Research*, 30(4), 879–890. <https://doi.org/10.1029/93WR03245>

- Uchida, T., & Asano, Y. (2010). Spatial variability in the flowpath of hillslope runoff and streamflow in a meso-scale catchment. *Hydrological Processes*, 24(16), 2277–2286. <https://doi.org/10.1002/hyp.7767>
- Uchida, T., Asano, Y., Ohte, N., & Mizuyama, T. (2003). Seepage area and rate of bedrock groundwater discharge at a granitic unchanneled hillslope. *Water Resources Research*, 39(1), 1018. <https://doi.org/10.1029/2002WR001298>
- Uchida, T., Miyata, S., & Asano, Y. (2008). Effects of the lateral and vertical expansion of the water flowpath in bedrock on temporal changes in hillslope discharge. *Geophysical Research Letters*, 35, L15402. <https://doi.org/10.1029/2008GL034566>
- Waseda, A., & Nakai, N. (1983). Isotopic compositions of meteoric and surface waters in Central and Northeast Japan. *Chikyukagaku*, 17(2), 83–91. <https://doi.org/10.14934/chikyukagaku.17.83>
- Way, J. H. (1972). *A more detailed discussion of the depositional environmental analysis: Middle and Upper Devonian sedimentary rocks, Catskill Mountain area, New York* (PhD dissertation). Troy, NY: Rensselaer Polytechnic Institute.
- Wood, E. F. (1995). Scaling behavior of hydrological fluxes and variables: Empirical studies using a hydrological model and remote-sensing data. *Hydrological Processes*, 9(3–4), 331–346. <https://doi.org/10.1002/hyp.3360090308>
- Wood, E. F., Sivapalan, M., Beven, K., & Band, L. (1988). Effects of spatial variability and scale with implications to hydrologic modeling. *Journal of Hydrology*, 102(1–4), 29–47. [https://doi.org/10.1016/0022-1694\(88\)90090-X](https://doi.org/10.1016/0022-1694(88)90090-X)
- Woods, R., Sivapalan, M., & Duncan, M. (1995). Investigating the representative elementary area concept—An approach based on field data. *Hydrological Processes*, 9(3–4), 291–312. <https://doi.org/10.1002/hyp.3360090306>
- Yamada, T., Hibino, T., Arai, T., & Nakatsugawa, M. (1995). Statistical characteristics of rainfall in mountainous basins. *Journal of Japan Society of Civil Engineers*, 527, 1–13. https://doi.org/10.2208/jscej.1995.527_1 (in Japanese with English abstract)
- Yamanaka, T., Makino, Y., Wakiyama, Y., Kishi, K., Maruyama, K., Kano, M., & Suzuki, K. (2015). How reliable are modeled precipitation isoscapes over a high-relief mountainous region? *Hydrological Research Letters*, 9(4), 118–124. <https://doi.org/10.3178/hrl.9.118>
- Yamanaka, T., Suzuki, K., Wakiyama, Y., Kishi, K., Makino, Y., Maruyama, K., & Yoshitake, S. (2016). Isotope mapping on mountainous regions: Current state and way forward. *Journal of Japanese Association of Hydrological Sciences*, 46(2), 73–86. <https://doi.org/10.4145/jahs.46.73>
- Zimmer, M. A., & Gannon, J. P. (2018). Run-off processes from mountains to foothills: The role of soil stratigraphy and structure in influencing run-off characteristics across high to low relief landscapes. *Hydrological Processes*, 32(11), 1546–1560. <https://doi.org/10.1002/hyp.11488>

Reference From the Supporting Information

- Geological Survey of Japan, AIST. (2015). Seamless digital geological map of Japan 1: 200,000. May 29, 2015 version. Geological Survey of Japan, National Institute of Advanced Industrial Science and Technology.